Cardiovasc Intervent Radiol (2012) 35:661–667
DOI 10.1007/s00270-011-0192-0

LABORATORY INVESTIGATION

A Signal-Inducing Bone Cement for Magnetic Resonance Imaging-Guided Spinal Surgery Based on Hydroxyapatite and Polymethylmethacrylate

Florian Wichlas · Christian J. Seebauer · Rene Schilling · Jens Rump · Sascha S. Chopra · Thula Walter · Ulf K. M. Teichgräber · Hermann J. Bail

Received: 6 April 2011 / Accepted: 11 May 2011 / Published online: 1 June 2011

Abstract The aim of this study was to develop a signal-inducing bone cement for magnetic resonance imaging (MRI)–guided cementoplasty of the spine. This MRI cement would allow precise and controlled injection of cement into pathologic lesions of the bone. We mixed conventional polymethylmethacrylate bone cement (PMMA; 5 ml methylmethacrylate and 12 g polymethylmethacrylate) with hydroxyapatite (HA) bone substitute (2–4 ml) and a gadolinium-based contrast agent (CA; 0–60 µl). The contrast-to-noise ratio (CNR) of different CA doses was measured in an open 1.0-Tesla scanner for fast T1W Turbo-Spin-Echo (TSE) and T1W TSE pulse sequences to determine the highest signal. We simulated MRI-guided cementoplasty in cadaveric spines. Compressive strength of the cements was tested. The highest CNR was (1) 87.3 (SD 2.9) in fast T1W TSE for cements with 4 µl CA/ml HA (4 ml) and (2) 60.8 (SD 2.4) in T1W TSE for cements with 1 µl CA/ml HA (4 ml). MRI-guided cementoplasty in cadaveric spine was feasible. Compressive strength decreased with increasing amounts of HA from 46.7 MPa (2 ml HA) to 28.0 MPa (4 ml HA). An MRI-compatible cement based on PMMA, HA, and CA is feasible and clearly visible on MRI images. MRI-guided spinal cementoplasty using this cement would permit direct visualization of the cement, the pathologic process, and the anatomical surroundings.

Keywords Cementoplasty · Vertebroplasty · PMMA bone cement · MRI · Contrast agent · Hydroxyapatite

F. Wichlas (✉) · C. J. Seebauer · R. Schilling · S. S. Chopra · H. J. Bail
Center for Musculoskeletal Surgery, University Charité, 13353 Berlin, Germany
e-mail: florian.wichlas@charite.de

J. Rump · T. Walter · U. K. M. Teichgräber
Department of Radiology, University Charité, 13353 Berlin, Germany

Introduction

Magnetic resonance imaging (MRI) is indispensable in the planning of spinal cancer surgery. Tumors, metastases, and especially pathologic fractures of the spine, neoplastic or not, are clearly visible on MRI [1]. Tumor infiltration of the surrounding tissues can be quantified, and therapeutic decisions can be made. In fractures, fracture plane and edema can be analyzed, and the age of the fracture can thus be determined. The same comprehensive information on the pathology cannot be matched by any diagnostic tool using x-ray [2]. MRI-guided musculoskeletal interventions have been proven to be feasible [3]. The detection of soft tissues and other delicate structures, such as nerves, vessels, and spinal cord, improves the safety of these interventions [4]. Fast interventional MRI-sequences generate short repetition rates and allow real-time imaging during the intervention.

To ensure feasible MRI-guided interventions, dedicated MRI-compatible instruments and materials must be developed for such procedures [5]. Currently these instruments are identified indirectly, by the lack of signal because MRI can only visualize protons, i.e., water. Signal-inducing materials are advantageous for such interventions.

Because cementoplasty is considered the standard treatment for most pathological spinal fractures, whether osteoporotic or neoplastic [6–8], simultaneous visualization of the cement and the pathologic lesion is beneficial

during the cement's injection. In** kyphoplasty, in which a bone cavity lacks signal results, the cement's signal would permit a controlled defect-filling.

Hydroxyapatite (HA)-based bone substitutes contain water for MRI signal and have an osteoconductive potential [9]. They provide a biologic bone–cement interface [10], and mixing them with conventional polymethylmethacrylate cements (PMMA) increases bioavailability of the PMMA [11].

A contrast agent (CA) further enhances the MRI signal of the PMMA–HA compound.

The aim of this study was to develop and analyze an MRI signal–inducing bone cement based on PMMA, HA, and CA mixture. The signal properties and the compressive strength of this cement were assessed.

Materials and Methods

PMMA (Bon Os; aap Biomaterials, Dieburg, Germany) is made up of a powdery polymer (12 g polymethylmethacrylate) and a liquid monomer (5 ml methylmethacrylate) and cures after mixing. We added 4 ml HA (Ostim 35; aap Biomaterials) and a gadolinium-based CA (0.5 mmol/ml Dotarem [gadoterate meglumine]; Guerbet, Paris, France) to the cement. First the CA was added to the HA; then the two components were mixed with the PMMA in a plastic cup with a spatula.

Signal Evaluation

We evaluated the cement's signal with increasing CA concentrations (0–60 µl gadoterate meglumine/mm HA) in the cement compound. The added increments of CA were 0.5, 1, 1.5, 2, 4, 10, 15, 20, 30, 40, and 60 µl. To determine the amount of HA necessary for an adequate signal, we decreased the HA in 1-ml increments from 4 to 2 ml using CA concentrations of 1 and 4 µl/ml HA. We tested the cured cements 24 h after mixing, in 10-ml sealed syringes, which were placed into a rack of a double-walled Plexiglas box. The space in between the box's walls was filled with water and served as a reference signal. We tested five specimens of each cement composition as follows:

- Two milliliters HA + 5 ml methylmethacrylate + 12 ml polymethylmethacrylate + CA µl (0.5/1/1.5/2/4/10/15/20/30/40/60 µl)
- Three milliliters HA + 5 ml methylmethacrylate + 12 ml polymethylmethacrylate + CA µl (0.5/1/1.5/2/4/10/15/20/30/40/60 µl)
- Four milliliters HA + 5 ml methylmethacrylate + 12 ml polymethylmethacrylate + CA µl (0.5/1/1.5/2/4/10/15/20/30/40/60 µl)

Applicability in the Spine

We tested the cement's applicability in cadaveric human spines by simulating vertebroplasty. This procedure should prove general feasibility, which can hardly be quantified. In addition, it should answer some critical questions such as the following: Can the MRI cement be injected from a conventional 5-ml syringe through the vertebroplastic needle in the vertebral body? Is the cement's visibility sufficient in the fast T1W Turbo-Spin-Echo (TSE) pulse sequences, and is the image-repetition rate fast enough? Are there any artifacts that hinder the procedure? Finally, it should rule out unforeseen adverse events. The cement was injected transpedicularly with an MRI-compatible vertebroplastic needle (Somatex Medical Technologies, Teltow, Germany) in 20 vertebral bodies from 4 lumbar spines (all female) with surrounding muscle and soft tissue. The spines' ages were 82, 87, 88, and 88 years. The needle had an outer diameter of 3.0 mm, an inner diameter of 2.45 mm, and a length of 100 mm. A 5-ml syringe was used to inject cement into the vertebral bodies under MRI guidance in an open high-field MRI scanner. The injected cement was made up of 3 ml HA, 4 µl CA, and PMMA. Because the CNRs between cement and bone are reproducibly measurable, they were the only hard data recorded (see later text).

Measurements in the Open MRI

The cement was scanned in an open high-field MRI (1.0-Tesla Panorama; Philips Medical System, Eindhoven, The Netherlands). Because CAs are T1 specific, we used T1-weighted (T1W) fast (turbo) spin echo pulse sequences for the scans. The pulse sequences were an interventional fast T1W TSE (TR 100 ms, TE 5 ms, α 110°, slice thickness 5 mm) and a T1W TSE (TR 400 ms, TE 10 ms, α 90°, slice thickness 4 mm) sequence. The spinal interventions were conducted under image control with fast T1W TSE sequences. The fast sequence had an acquisition time of 2.6 s**,** and the image orientation was flipped alternately 90° between a sagittal and an axial plane. All images were evaluated without postprocessing or image filters.

The scans of the cement specimens were performed with a solenoid head coil and those of the spinal specimens with an interventional surface coil (multipurpose L). The MRI signal was evaluated by determining the CNR of the cement to air (CNR^{Air}) and to bone (CNR^{Bone}). CNR is calculated by measuring the cement's image signal in the region-of-interest, the surrounding's image signal (background), and the SD of the background noise as described by Hendrick [12]. We defined equal areas (20 × 20 pixels, 133 mm^2) in the cements and their surroundings and measured the signal in eight slices per specimen for five specimens of each cement composition. Due to lower amounts of cement in the

vertebral bodies, we measured only three slices for five specimens. The CNR^{Air} was plotted over the CA concentration to determine the maximal MRI signal.

Compressive Strength

Different amounts of HA (2, 3, and 4 ml) were added to the PMMA to evaluate the compressive strength of the cement. Standard PMMA served as the control group. Ten microliters of CA/ml HA were added to the cements for testing because the amounts for optimal signal are smaller (see Results). We tested compressive strength in accordance with the International Organization for Standardization with the method described in ISO 5833:2002 (E) [13]. The cements were filled in different cylindrical polytetrafluoroethylene forms and stored under standardized environmental conditions (23°C [SD 1°C]) for at least 2 h before testing as follows:

- Two milliliters HA + 5 ml methylmethacrylate + 12 ml polymethylmethacrylate + 10 µl CA
- Three milliliters HA + 5 ml methylmethacrylate + 12 ml polymethylmethacrylate + 10 µl CA
- Four milliliters HA + 5 ml methylmethacrylate + 12 ml polymethylmethacrylate + 10 µl CA

The PTFE forms were 12-mm long (SD 0.1 mm) and 6 mm in diameter (SD 0.1 mm). The cured specimens were visually controlled for trapped air or surface defects, polished, and then packed into aluminum bags to avoid dehydration. After being conditioned for 24 h (SD 2 h) at 23°C (SD 1°C), the cements were compressed on an Instron universal testing-machine (Instron no. 3366; Norwood, MA). The specimens were placed upright between the platens and compressed at a rate of 22.70 mm/min until failure occurred. The compressive strength at maximum load or at 2% offset load of the upper yield point, whichever occurred first, were determined. Compressive strength (MPa) and modulus of elasticity were calculated for 6 specimens. The compressive strength was calculated according to formulas provided in the ISO specifications.

Results

The MRI cement's manufacturing was feasible and similar to that of conventional PMMA. Because PMMA is hydrophobic and the added HA is water-based, the compound requires at least 2 min of stirring until the PMMA–HA–CA mixture is homogenous.

Signal Evaluation

The signal (CNR^{Air}) of the cement depended on the CA concentration, the amount of HA, and the pulse sequence used (Figs. 1, 2, 3; Table 1). The CNR^{Air} curve had the typical sequence-dependent shape of paramagnetic substances showing a signal increase up to a maximum

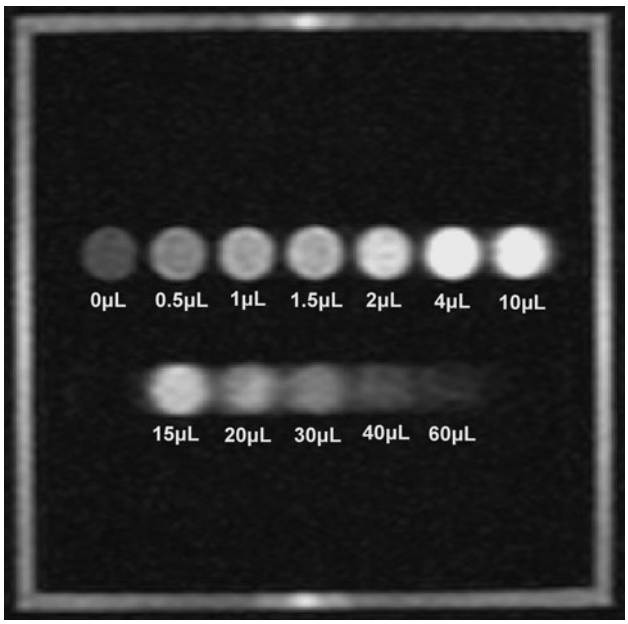

Fig. 1 Rack of cement-filled syringes in fast T1W TSE. CA was dosed from 0 to 60 µl/ml HA in 4 ml HA, 5 ml methylmethacrylate, and 12 g polymethylmethacrylate. The pulse-sequence was fast T1W TSE, and a head coil was used. Gadoterate meglumine doses were 0, 0.5, 1, 1.5, 2, 4, 10, 15, 20, 30, 40, and 60 µl

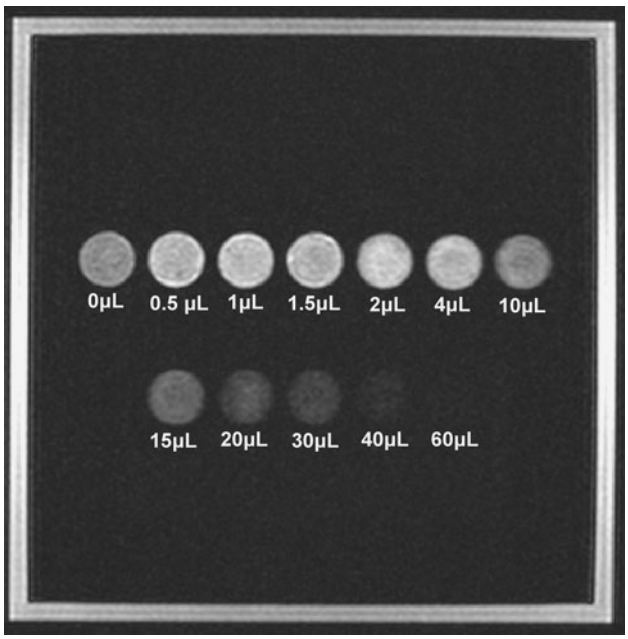

Fig. 2 Rack of cement-filled syringes in T1W TSE. CA was dosed from 0 to 60 µl/ml HA in 4 ml HA, 5 ml methylmethacrylate, and 12 g polymethylmethacrylate. The pulse-sequence was T1W TSE, and a head coil was used. Gadoterate meglumine doses were 0, 0.5, 1, 1.5, 2, 4, 10, 15, 20, 30, 40, and 60 µl

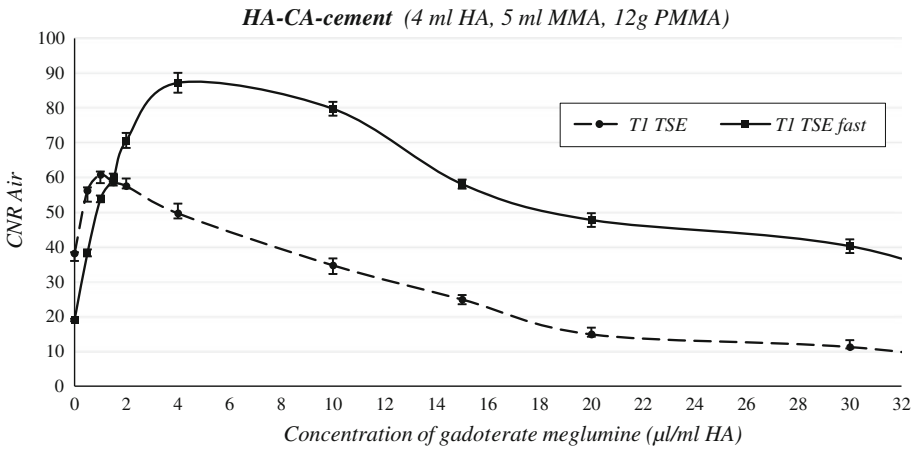

Fig. 3 CNR^{Air} of cements in T1W TSE and fast T1W TSE. Data are from the cement racks in Figures. 1 and 2. CNR^{Air} represents contrast to the surrounding air. Gadoterate meglumine was dosed in µl per ml HA in 4 ml HA, 5 ml methylmethacrylate, and 12 g polymethylmethacrylate

Table 1 CNR^{Air} and compressive strength based amount of HA added to PMMA[a]

HA in cement (ml)	CNR^{Air} in T1W TSE for 1 µl gad meg/ml HA	CNR^{Air} in fast T1W TSE for 4 µl gad meg/ml HA	Compressive strength (MPa)
0	–	–	84.6 ± 5.3
2 (13.8%)	27.3 ± 0.7	38.1 ± 5.3	46.7 ± 0.8
3 (19.4%)	49.5 ± 1.1	53.2 ± 4.5	36.9 ± 2.0
4 (24.2%)	60.8 ± 2.4	87.3 ± 2.9	28.0 ± 1.9

Gad meg Gadoterate meglumine

[a] Two to four milliliters HA were added to the cement (5 ml methylmethacrylate and 12 g polymethylmethacrylate). One microliter gad meg/milliliter HA was added to the compound in T1W TSE, and 4 µl was added in fast T1W TSE. Compressive strength is measured in MPa for these cements (2–4 ml HA, 5 ml methylmethacrylate, 12 g polymethylmethacrylate, and 10 µl CA/ml HA). Percentages express the amount of HA in the total compound

followed by a decrease to signal extinction [14]. Fast T1W TSE sequences had greater peaks at different CA concentrations than standard T1W TSE. The maximal CNR^{Air} in fast T1W TSE was 87.3 (SD 2.9) for cements with 4 µl CA/ml HA (16 µl gadoterate meglumine [4 ml HA]). In T1W TSE, CNR^{Air} was 60.8 (SD 2.4) for cements with 1 µl CA/ml HA (4 µl gadoterate meglumine [4 ml HA]). A decreasing amount of HA (4–2 ml) resulted in relatively linear signal loss (Table 1).

Applicability in the Spine

The MRI-guided cement injection into the vertebral body through a vertebroplastic needle was feasible (Fig. 4). Injection with a 5-ml syringe through the vertebroplastic provided sufficient pressure. The cement's signal and contrast to air and to bone were clear. The exact detection of the cement permitted controlled injection and visualization of the procedure under the fast T1W TSE guidance. The CNR^{Bone} in fast T1W TSE images was 11.8 (SD 0.1). The cement injection speed had to be adapted to the frame rate of 2.6 s to control the injection. This acquisition time provided sufficient resolution of skeletal structures and soft tissues. The needle's artifacts were strictly limited to the needle itself and did not disturb the procedure. After injection, the CNR^{Bone} in T1W TSE images was 30.7 (SD 7.5).

Compressive Strength

Increasing the amount of HA resulted in lower compressive strength (Table 1). Although the first 2 ml HA reduced the initial compressive strength of conventional PMMA for nearly 50 percent, every further ml HA decreased the strength for only 10 MPa.

Discussion

In this study, we found that it is possible to induce an adequate MR-signal in PMMA bone cements with HA and CA. The main principle to induce an MRI signal in PMMA cement is to mix it with water (protons) and CA.

The signal intensity of the MRI cement can be manipulated by changing the amount of HA, the amount of CA, or the pulse sequence. These physical variables determine the signal. Pulse sequences can be modified by the MRI user to maximize the signal in the region of interest [15].

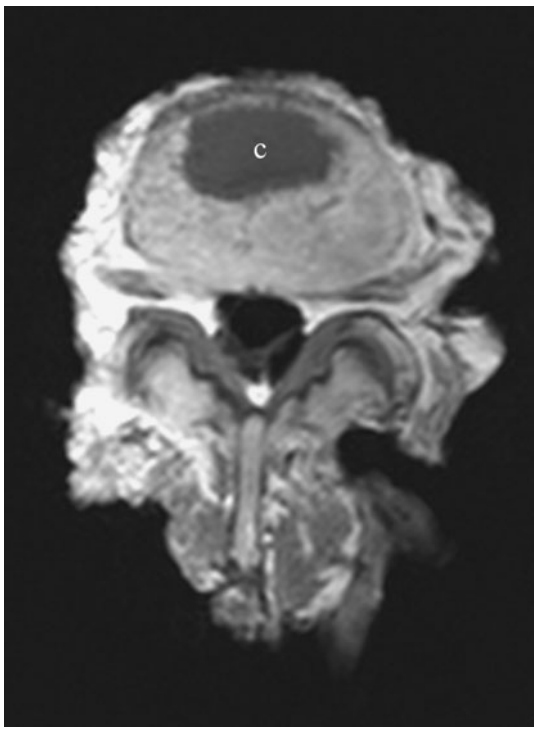

Fig. 4 Transversal vertebral body after cement filling in T1W TSE. The cement consisted of 4 µl gadoterate meglumine, 4 ml HA, 5 ml methylmethacrylate, and 12 g polymethylmethacrylate. The pulse-sequence was T1W TSE, and a body coil was used. C = cement

The MRI signal depends linearly on the amount of HA due to the amount of protons. Every CA has its own signal peak before extinction occurs depending on its paramagnetic properties [16]. Both substances are essential in gaining the maximum signal.

Among the existing CAs, gadolinium induces the highest MRI signal [17]. However, there has been some concern about the use of gadolinium due to cases of nephrogenic systemic fibrosis [18]. Despite the fact that we used gadolinium in this study, generally any CA can be used in the cement to induce a signal; this MRI cement merely demonstrates the principle. Furthermore, toxicological thresholds of gadoterate meglumine were not reached with the miniscule doses used in this study [19]. We used gadolinium because it is readily available in our institution.

In this study, all MRI cements produced a clear signal. The CNR^{Bone} was smaller than the CNR^{Air} because the signal of bone is greater than the signal of air but was far greater than 4. According to the Rose model [20], CNR should be >4 to guarantee a sufficient contrast to the surrounding structures for visual differentiation. The high CNR^{Bone} permitted direct control of the injection procedure in cadaveric spines with fast T1W TSE, and visualization on T1W TSE images after the procedure. We focused on T1W sequences due to their CA sensitivity. In T2W sequences the MRI cements could be used as well, but the signals would have lower CNR peaks at different CA concentration [14].

Certainly, MRI-guided cementoplasty must be tested in a clinical setting to rule out unpredictable factors, such as patient breathing or other patient-dependent artifacts. Long-term testing is needed to investigate the cement's signal behavior over time and to determine whether the cement would be detectable in postoperative diagnostics in vivo.

Because PMMA is biologically inert, the cured cement is later surrounded by a biomembrane within the bone, as is typical for foreign bodies [21]. Hydroxyapatite has better biocompatibility [22, 23], which leads to its increased application for cementoplasty [24]. In our study, HA are hydroxyapatite crystals as a suspension in water, which can easily be mixed with PMMA. HA contains enough water to generate an MRI signal and has a better biocompatibility than conventional polymethylmethacrylate cement. Thus, HA seems to be the ideal additive for PMMA.

The increasing amount of HA decreases the compressive strength. The mechanical properties of cements have been discussed in the literature extensively [25], but their outcomes remain inconclusive. The results among the different studies on the fracture risk after vertebroplasty and kyphoplasty remain controversial. Although some studies show a greater risk of adjacent spinal fractures after vertebroplasty and kyphoplasty [26], but others do not [27]. It is unclear how strong a cement must be [28] be safe for clinical application. The compressive strength is the main factor for the design of kyphoplastic and vertebroplastic cements and is quite often the only tested parameter [29]. Calcium phosphate cements, which are currently being used for cementoplasty, have compressive strengths of 70 MPa [30] in vitro; however, in an aqueous environment they only withstand 5–25 MPa [31]. The MRI cement matches these values for all amounts of HA (2–4 ml) added to the PMMA. Although the properties of bone cements used in spinal surgery should be determined, dynamic long-term tests are needed to show the MRI cement's clinical applicability.

The increasing amount of HA impairs the cement's compressive strength but increases the cement's MRI signal. A high MRI signal requires high amounts of HA; a mechanical resistant one requires low amounts. This means that the signal's advantage of an increasing HA amount is limited by the mechanical disadvantage. Because the cement's compressive strength is the crucial parameter for cementoplasty, we suggest a PMMA cement (5 ml methylmethacrylate + 12 ml polymethylmethacrylate) containing 2–3 ml HA with 8–12 µl gadolinium for cementoplasty.

Our results support what has been shown earlier for the enhancement of CA in MRI [32]: A CA

concentration-dependant signal curve in the MRI-cements. Concerning the biomechanical properties, the results of the mechanical tests of HA–PMMA compounds support the published data [33] and advocate their use due to their better biocompatibility [34].

Along with the increasing availability of MRI, preoperative MRI diagnostics of the spine increase [35, 36] and the number of MRI-guided interventions is growing [37]. MRI-guided surgery is limited by the dictates of MRI sequences, the induced instrument artifacts and MRI safety. The present MRI-cement overcomes these limitations, as it is MR safe, induces its own signal, and is not visualized as an artifact. In the treatment of neoplasms or fractures with MRI-guided cementoplasty, direct visualization of the pathology and the anatomical structures is possible throughout the procedure. This enables control of the cement, visualization of the neoplasm or fracture and spinal structures, such as nerves, vessels, and soft tissues during the cement application. Furthermore, the cement's high signal increases safety because it prevents cement leakage. Indirect visualization of the cement would only detect the compression of soft tissues and structures at risk approximately the vertebral body.

MRI-guided interventions allow the treatment of pathologic lesions, which are not detectable with conventional imaging under direct visualization. MRI cement is necessary because MRI-guided cementoplasty requires clearly visible cement [38], which can be differentiated from the surrounding structures. This cement would allow precise and controlled injection of cement into pathologic lesions of the bone, thereby increasing the precision of MRI-guided cementoplasty. In bone-defect filling, such as kyphoplasty, the cement's signal becomes crucial because it permits complete filling.

Although the resolution of real-time imaging is improving rapidly, and frame rates are becoming shorter, image quality must be improved further to warrant the precision of MRI-guided interventions. A fast-moving grid sequence should be developed to generate a three-dimensional picture of the region of interest. Sequence modulation, such as spectral fat saturation inversion recovery sequences, could further improve the cement's visibility by suppressing the bone marrow's signal and thereby increasing the contrast.

In the future, this MRI-compatible cement could broaden the field of MRI-guided cementoplasty to the treatment of other osseous neoplasms to provide both ideal intervention control and postinterventional follow-up.

Conclusion

We developed a PMMA-based signal-inducing bone cement with HA and CA the use in MRI interventional procedure. The cement produces a clearly detectable MRI signal and equals the compressive strength of existing cements for spinal cementoplasty.

Acknowledgments This project was financed by TSB Technologiestiftung Berlin–Zukunftsfonds Berlin and cofinanced by the European Union–European Fund for Regional Development (Project No. 10132816/10134231). The mechanical tests were performed at aap Biomaterials, Dieburg, Germany. We thank Christoph Sattig and Nora Lämmel from aap Biomaterials for their valuable contributions.

Conflict of interest The authors declare that they have no conflict of interest.

References

1. Hwang S, Panicek DM (2009) The evolution of musculoskeletal tumor imaging. Radiol Clin North Am 47:435–453
2. Buhmann Kirchhoff S, Becker C, Duerr HR et al (2009) Detection of osseous metastases of the spine: comparison of high resolution multi-detector-CT with MRI. Eur J Radiol 69:567–573
3. Carrino JA, Blanco R (2006) Magnetic resonance–guided musculoskeletal interventional radiology. Semin Musculoskelet Radiol 10:159–174
4. Smith KA, Carrino J (2008) MRI-guided interventions of the musculoskeletal system. J Magn Res Imaging 27:339–346
5. Shellock FG (2001) Metallic surgical instruments for interventional MRI procedures: evaluation of MR safety. J Magn Res Imaging 13:152–157
6. Anselmetti GC, Corrao G, Monica PD et al (2007) Pain relief following percutaneous vertebroplasty: results of a series of 283 consecutive patients treated in a single institution. Cardiovasc Intervent Radiol 30(3):441–447
7. Quraishi NA, Gokaslan ZL, Boriani S (2010) The surgical management of metastatic epidural compression of the spinal cord. J Bone Joint Surg Br 92(8):1054–1060
8. Anselmetti GC, Manca A, Montemurro F et al (2011) Percutaneous vertebroplasty in multiple myeloma: prospective long-term follow-up in 106 consecutive patients. Cardiovasc Intervent Radiol [Epub ahead of print]
9. Meyer S, Floerkemeier T, Windhagen H (2007) Histological osseointegration of a calciumphosphate bone substitute material in patients. Bio-Med Mater Eng 17:347–356
10. Hernández L, Parra J, Vázquez B et al (2009) Injectable acrylic bone cements for vertebroplasty based on a radiopaque hydroxyapatite: bioactvity and biocompatibility. J Biomed Mater Res B Appl Biomater 88:103–114
11. Kim SB, Kim YJ, Yoon TL et al (2004) The characteristics of a hydroxyapatite-chitosan-PMMA bone cement. Biomaterials 25(26):5715–5723
12. Hendrick RE (2008) Signal, noise, signal-to-noise, and contrast-to-noise ratios. In: Hendrick RE (ed) Breast MRI: fundamentals and technical aspects. Springer, New York, NY, pp 93–111
13. Implants for surgery Acrylic resin cements (2002) In: International standard ISO 5833. 2nd edn, pp 15–19
14. Hendrick RE, Haacke EM (1993) Basic physics of MR contrast agents and maximization of image contrast. J Magn Res Imaging 3:137–148
15. Elster AD (2008) How much contrast is enough? Dependence of enhancement on field strength and MR pulse sequence. Eur Radiol 1997(Suppl 7)5:276–280
16. Geraldes CF, Laurent S (2009) Classification and basic properties of contrast agents for magnetic resonance imaging. Contrast Media Mol Imaging 4(1):1–23

17. Runge VM (2008) Notes on „Characteristics of gadolinium-DTPA complex: a potential NMR contrast agent.". AJR Am J Roentgenol 190(6):1433–1434
18. Van der Molen AJ (2008) Nephrogenic systemic fibrosis and the role of gadolinium contrast media. J Med Imaging Radiat Oncol 52:339–350
19. Bussi S, Fouillet X, Morisetti A (2007) Toxicological assessment of gadolinium release from contrast media. Exp Toxicol Pathol 58:323–330
20. Rose A (1973) Vision: human and electronic. Plenum, New York, NY
21. Kuehn KD, Ege W, Gopp U (2005) Acrylic bone cements: mechanical and physical properties. Orthop Clin North Am 36:29–39
22. Lewis G (2006) Injectable bone cements for use in vertebroplasty and kyphoplasty: state-of-the-art review. J Biomed Mater Res B Appl Biomater 76(2):456–468
23. Laschke MW, Witt K, Pohlemann T et al (2007) Injectable nanocrystalline hydroxyapatite paste for bone substitution: in vivo analysis of biocompatibility and vascularization. J Biomed Mater Res B Appl Biomater 82:494–505
24. Lieberman IH, Togawa D, Kayanja MM (2005) Vertebroplasty and kyphoplasty: filler materials. Spine J 5(Suppl 6):305S–316S
25. Nouda S, Tomita S, Kin A et al (2009) Adjacent vertebral body fracture following vertebroplasty with polymethylmethacrylate or calcium phosphate cement: biomechanical evaluation of the cadaveric spine. Spine 15:2613–2618
26. Mudano AS, Bian J, Cope JU et al (2009) Vertebroplasty and kyphoplasty are associated with an increased risk of secondary vertebral compression fractures: a population-based cohort study. Osteoporos Int 20:819–826
27. Taylor RS, Fritzell P, Taylor RJ (2007) Balloon kyphoplasty in the management of vertebral compression fractures: an updated systematic review and meta-analysis. Eur Spine J 16:1085–1100
28. Wilke HJ, Mehnert U, Claes LE et al (2006) Biomechanical evaluation of vertebroplasty and kyphoplasty with polymethyl methacrylate or calcium phosphate cement under cyclic loading. Spine 1:2934–2941
29. Nottrott M, Mølster AO, Moldestad IO et al (2008) Performance of bone cements: are current preclinical specifications adequate? Acta Orthop 79:826–831
30. Belkoff SM, Mathis JM MD, Jasper LE et al (2001) An ex vivo biomechanical evaluation of a hydroxyapatite cement for use with vertebroplasty. Spine 26:1542–1546
31. Bermudez O, Boltong MG, Driessens FCM et al (1993) Compressive strength and diametral tensile strength of some calcium-orthophosphate cements: a pilot study. J Mater Sci Mater Med 4:389–393
32. Kirsch JE (1991) Basic principles of magnetic resonance contrast agents. Top Magn Reson Imaging 3(2):1–18
33. Ishihara K, Arai H, Nakabayashi N et al (1992) Adhesive bone cement containing hydroxyapatite particle as bone compatible filler. J Biomed Mater Res 26:937–945
34. Itokawa H, Hiraide T, Moriya M et al (2007) A 12 month in vivo study on the response of bone to a hydroxyapatite–polymethylmethacrylate cranioplasty composite. Biomaterials 28:4922–4927
35. Spiegl UJA, Beisse R, Hauck S et al (2009) Value of MRI imaging prior to a kyphoplasty for osteoporotic insufficiency fractures. Eur Spine J 18:1287–1292
36. Masala S, Massari F, Assako OP et al (2010) Is 3T-MR spectroscopy a predictable selection tool in prophylactic vertebroplasty? Cardiovasc Intervent Radiol 33(6):1243–1252
37. Kim JH, Kang HG, Kim HS (2010) MRI-guided navigation surgery with temporary implantable bone markers in limb salvage for sarcoma. Clin Orthop Relat Res 468(8):2211–2217
38. Teng GJ, He SC, Deng G et al (2005) A simplified method of opacifying and mixing acrylic cement for percutaneous vertebroplasty: a clinical and in vitro study. Cardiovasc Intervent Radiol 28(5):570–577